A

EGFR;p53;Cas9 + osimertinib

		(11 weeks)		(19 weeks)	
		LN mean	*P*-value	LN mean	*P*-value
	sg*Rb1*	**1.87**	**<10^{-4}**	1.02	0.73
	sg*Rbm10*	**1.35**	**<10^{-4}**	**3.08**	**<10^{-4}**
	sg*Apc*	**1.49**	**<10^{-4}**	**2.08**	**0.001**
	sg*Smad4*	1.03	0.35	0.81	0.05
	sg*Keap1*	**1.41**	**<10^{-4}**	**2.06**	**0.04**
	sg*Atm*	0.98	0.51	0.95	0.50
	sg*Arid1a*	0.95	0.04	1.34	0.23
	sg*Cdkn2a*	1.03	0.15	**1.29**	**0.003**
	sg*p53*	1.00	0.85	0.90	0.67
	sg*Lkb1*	0.90	0.01	0.92	0.81
	sg*Setd2*	0.95	0.05	1.37	0.26
Inert	sg*Neo1*	1.01	0.74	0.89	0.05
Inert	sg*Neo2*	1.04	0.31	1.16	0.54
Inert	sg*Neo3*	0.99	0.66	**1.18**	**<10^{-4}**
Inert	sg*NT*	0.98	0.29	0.87	0.21

B

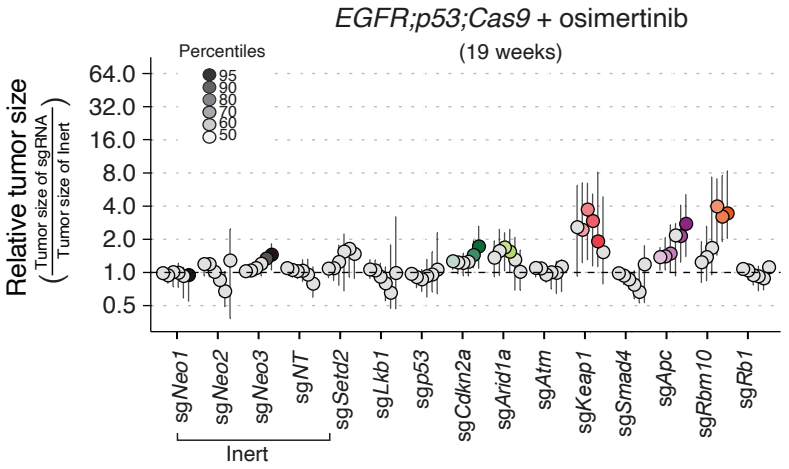

C

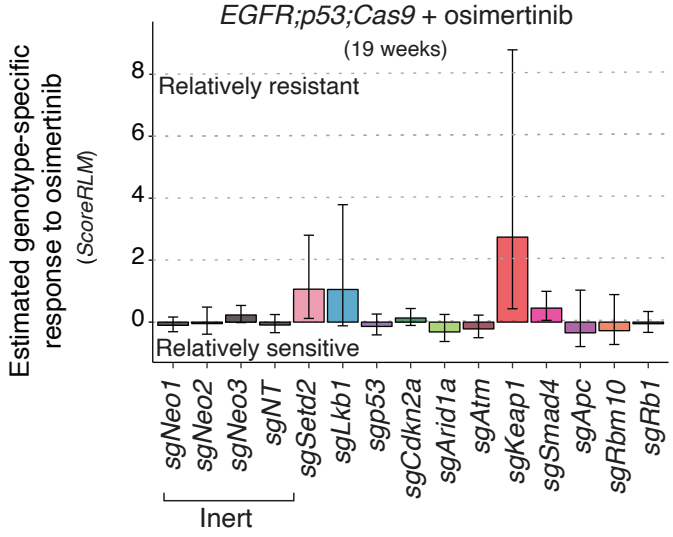

D

EGFR;p53;Cas9 + osimertinib (11 weeks)

		ScoreRGM		*ScoreRTN*	
		Score	*P*-value	Score	*P*-value
	sg*Rb1*	-0.38	0.06	0.01	0.37
	sg*Rbm10*	-0.15	0.33	0.12	0.20
	sg*Apc*	-0.16	0.23	-0.03	0.56
	sg*Smad4*	0.10	0.39	0.26	0.09
	sg*Keap1*	0.37	0.28	-0.02	0.64
	sg*Atm*	-0.12	0.21	-0.06	0.31
	sg*Arid1a*	0.02	0.58	-0.02	0.57
	sg*Cdkn2a*	-0.02	0.48	-0.08	0.39
	sg*p53*	0.06	0.30	0.03	0.43
	sg*Lkb1*	0.18	0.31	0.30	0.32
	sg*Setd2*	0.03	0.39	0.03	0.39
Inert	sg*Neo1*	0.02	0.41	0.01	0.50
Inert	sg*Neo2*	-0.02	0.47	0.00	0.64
Inert	sg*Neo3*	0.02	0.49	0.02	0.40
Inert	sg*NT*	-0.03	0.41	-0.02	0.40

E

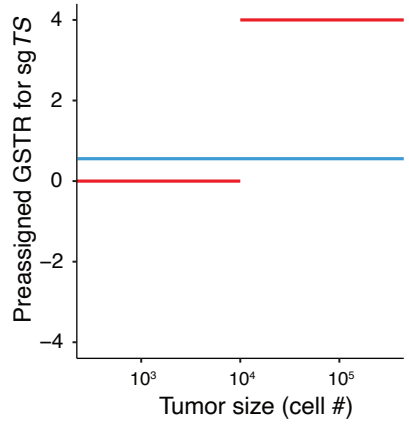

F

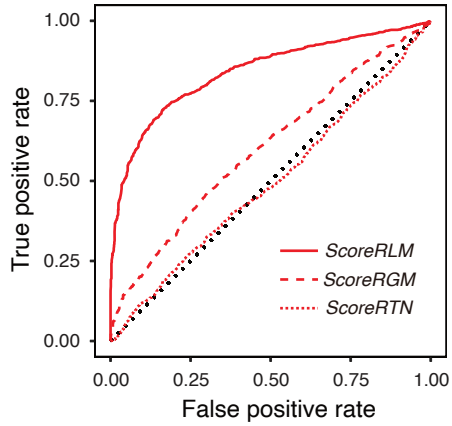

G

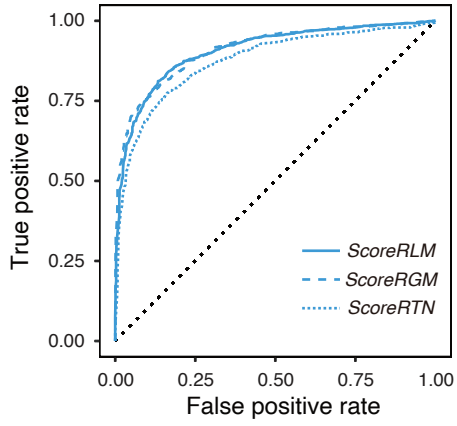

Supplementary Figure S11. *Keap1* inactivation limits sensitivity to treatment with osimertinib.

A. LN mean of osimertinib-treated tumors with each sgRNA normalized to inert tumors in *EGFR;p53;Cas9* mice at 11 and 19 weeks after tumor initiation. *P*-values were calculated from bootstrapping. *P*-values < 0.05 and their corresponding means are highlighted in red or green when the size effects are equal to or >10% compared to the size of tumors with inert sgRNAs.
B. Graph of the relative size of tumors of each genotype in *EGFR;p53;Cas9* mice ($n = 9$) 19 weeks after tumor initiation and 2 weeks of osimertinib treatment. The relative size of tumors at the indicated percentiles was calculated from the tumor size distribution of all tumors from nine mice. Error bars show the 95% confidence intervals. *P*-values were calculated from bootstrapping. Percentiles that are significantly different from the tumors with inert sgRNAs are in color.
C. Estimate of the genotype-specific treatment response (*ScoreRLM*) calculated by comparing the LN mean of tumors treated with osimertinib to the LN mean of vehicle-treated tumors in *EGFR;p53;Cas9* mice at 19 weeks of tumor initiation. Error bars indicate standard deviations. *P*-values were calculated from bootstrapping. None were significant, although *Keap1* inactivation is associated with a large magnitude of effect for decreased sensitivity.
D. Tabulation of two other metrics for genotype-specific responses based on the geometric mean (*ScoreRGM*) and the relative tumor number (*ScoreRTN*) do not show significant genotype-specific effects. *P*-values were calculated from bootstrapping.
E-G. Power analysis of each summary statistics (*ScoreRGM*, *ScoreRTN* and *ScoreRLM*) to uncover genotype-specific treatment responses (GSTRs). To generate tumor size profiles with known GSTRs, we generated simulated data from bootstrap resampling of *EGFR;p53;Cas9* vehicle-treated mice 11 weeks after tumor initiation ($n = 10$, from Fig. 2). We simulated an overall drug effect by reducing the size of all tumors in the simulated drug-treated group by 75%.
E. The red and blue lines show two examples of preassigned potential GSTRs on sgTS tumors. The red line represents a case where sg*TS* tumors larger than 10,000 cells do not respond to the drug at all, thus being 4-fold larger than expected without a GSTR (only the largest tumors show drug resistance). The blue line represents a case where all sg*TS* tumors were reduced in size by only 50%, thus being 50% larger than expected without a GSTR (equal resistance across all tumor sizes).
F. When identifying GSTRs as shown in the red lines in (**E**), *ScoreRTN* and *ScoreRGM* were much less sensitive than *ScoreRLM*.
G. When identifying GSTRs as shown in the blue line in (**G**), all three metrics showed reasonable and similar statistical power. Therefore, we used *ScoreRLM* as the summary statistic throughout this manuscript.

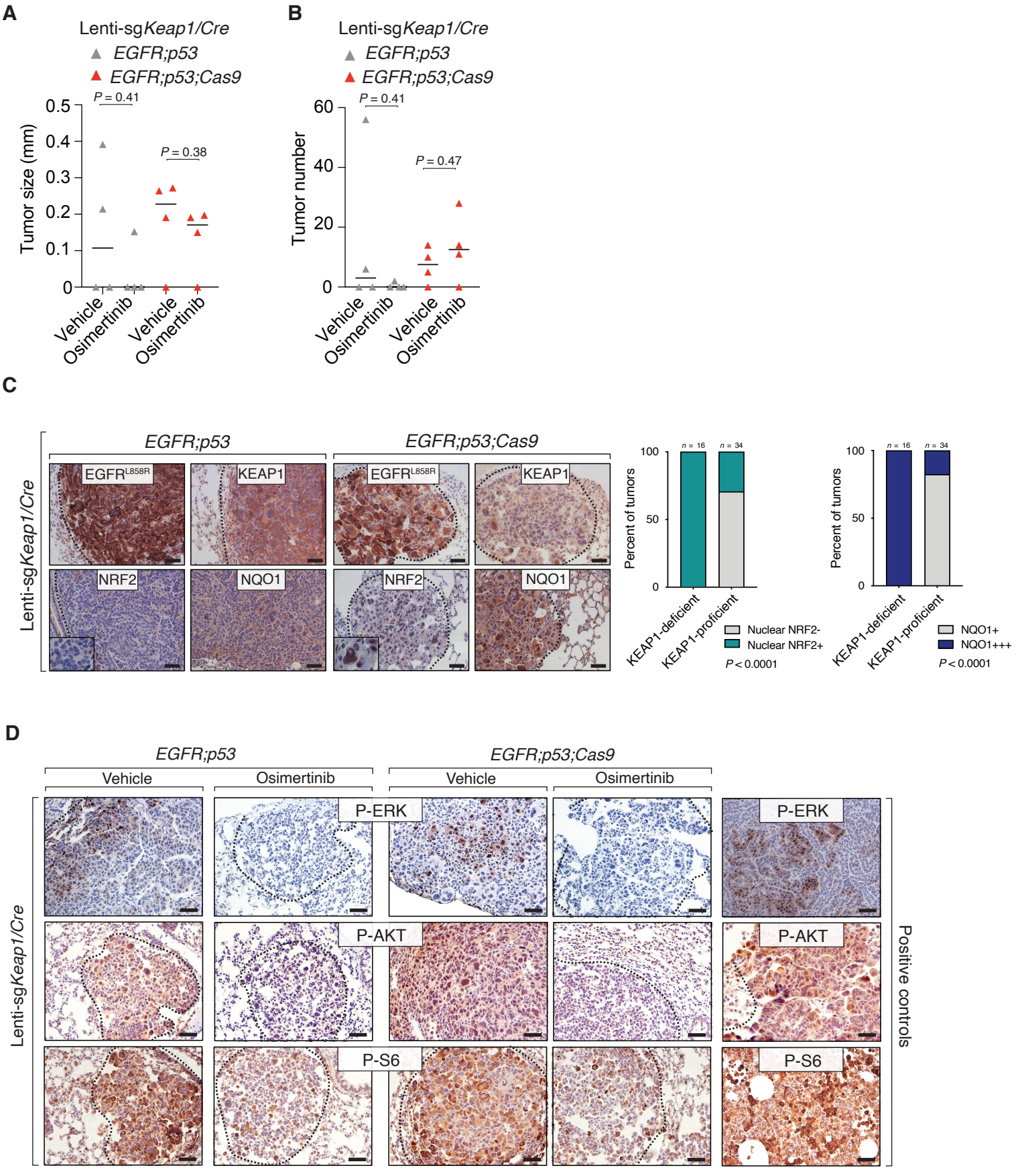

Supplementary Figure S12. Tumor size and number of tumors in vehicle- and osimertinib-treated tumors initiated with individual Lenti-sg*Keap1/Cre* virus.

Foggetti *et al.*

A. Graph of tumor size in *EGFR;p53* and *EGFR;p53;Cas9* mice with Lenti-sg*Keap1/Cre*-initiated tumors treated with either vehicle or osimertinib for 2 weeks (n = 4 mice-treated/group). Tumor size was calculated by measuring the longest diameter of each tumor in a histological lung section for each group. Each triangle represents the average of all the tumor sizes per mouse. *P*-values were calculated using the Mann-Whitney U test. Horizontal lines indicate the median.
B. Graph of tumor number in *EGFR;p53* and *EGFR;p53;Cas9* mice transduced with Lenti-sg*Keap1/Cre* virus and treated with either vehicle or osimertinib for 2 weeks. In both models, due to large mouse-to-mouse variations, tumor size and number comparisons between vehicle- and osimertinib-treated mice were not significantly different (Mann-Whitney U test). Each triangle represents the number of tumors in one lung section per mouse. Horizontal bars indicate the median.
C. Immunostaining for $EGFR^{L858R}$, KEAP1, NRF2 and NQO1 in *EGFR;p53* and *EGFR;p53;Cas9* mice with Lenti-sg*Keap1/Cre*-initiated tumors (left panels). The dashed lines indicate areas of tumors. Scale bars, 50 μm. Staining for NRF2 shows protein nuclear localization in KEAP1-deficient versus KEAP1-proficient tumors at higher magnification. Quantification of NRF2 nuclear expression and NQO1 expression levels in KEAP1-deficient versus KEAP1-proficient tumors arising in *EGFR;p53;Cas9* mice (right panels). *P*-values were calculated using a Chi-squared test.
D. Attenuation of MAPK/ERK and PI3K/AKT/mTOR signaling in *EGFR;p53;Cas9* tumors initiated with Lenti-sg*Keap1/Cre* upon osimertinib treatment. IHC for P-ERK and P-AKT, and P-Ribosomal protein S6 (P-S6) show decreased EGFR downstream signaling upon treatment with osimertinib for 2 weeks in *EGFR;p53* and *EGFR;p53;Cas9* tumors initiated with Lenti-sg*Keap1/Cre*. Scale bars, 50 μm. The positive controls were murine Kras- (P-ERK) and EGFR-driven lung adenocarcinomas (P-AKT and P-S6).

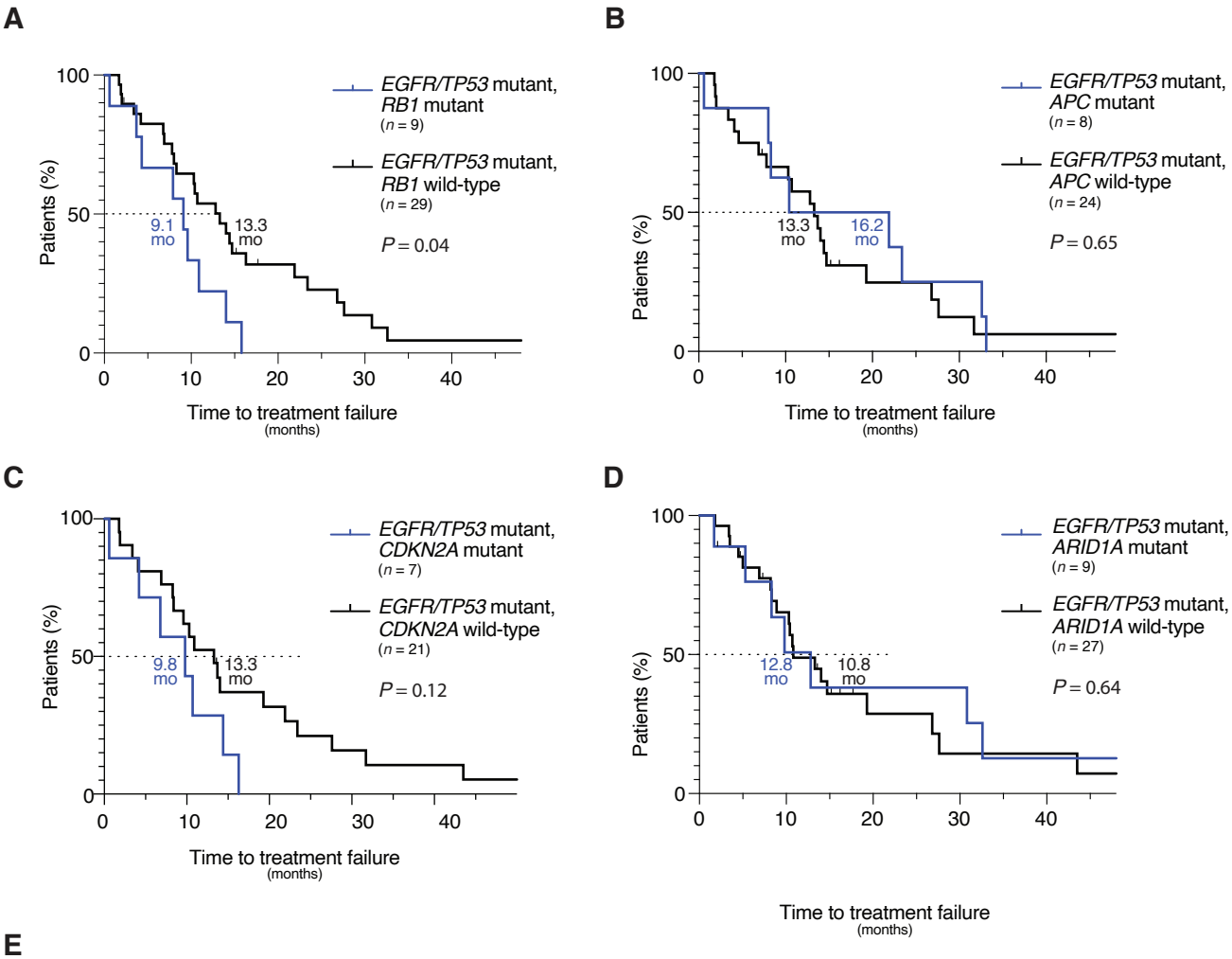

E

Source	*KEAP1*	*NFE2L2*	*CUL3*	TKI therapy	Reference
human data	loss (1/137)	n.d.	n.d.	AR to Erlotinib	Yu *et al.*, 2018
human data	n.a.	p.W24C (1/21)	n.a.	PD to Erlotinib/ NR to 2nd line Osimertinib	Blakely *et al.*, 2017
human data	n.d.	p.D321N (1/204)	p.N138S (1/204)	AR to Erlotinib	Jordan *et al.*, 2017
in vitro	loss	n.d.	n.d.	AR to Erlotinib	Krall *et al.*, 2017
in vitro	homozygous mutation (p.D236H)	n.d.	n.d.	AR to Gefitinib	Park *et al.*, 2018

Supplementary Figure S13. Mutations in tumor suppressor genes and time to TKI treatment failure in human EGFR-driven lung adenocarcinomas.
A-D. Kaplan-Meier curves showing time to TKI treatment failure in human mutant *EGFR/TP53* with mutations in *RB1* (**A**), *APC* (**B**), *CDKN2A* (**C**), *ARID1A* (**D**) compared to mutant *EGFR/TP53* cases without the corresponding genetic alterations. Time to treatment failure was determined by subtracting the date of discontinuation of TKI due to progression, toxicity or death, from the date of initiation of TKI. *P*-values were calcuated using the Log rank test.
E. Summary of existing literature on *KEAP1/NFE2L2/CUL3* alterations in human mutant *EGFR* lung adenocarcinomas, associated with progressive disease (PD) or acquired resistance (AR) to TKIs. *KEAP1* loss or missense mutations, and missense mutations in *NFE2L2* or *CUL3* have been observed (classified as pathogenic by COSMIC). For each reference, the number of cases, the type of alteration and the TKI therapeutic agent studied are indicated. n.a. = not analyzed. n.d. = not detected.

A

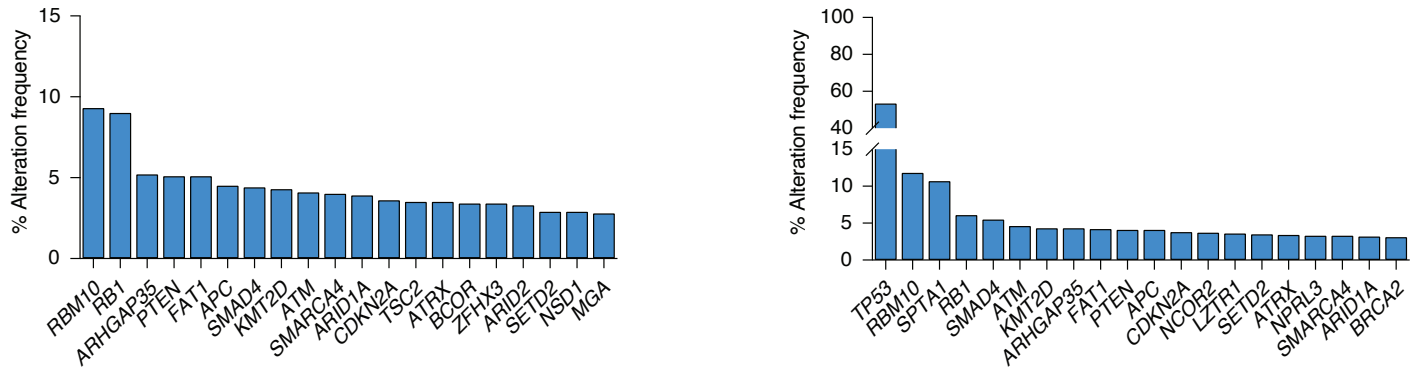

B

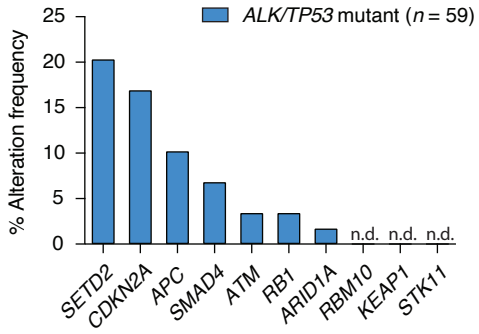

Supplementary Figure S14. Landscape of putative tumor suppressors gene mutations in lung cancer.
A. Mutational spectra in EGFR-driven lung adenocarcinomas (data from AACR Project GENIE). Frequency of the top 20 most commonly altered putative tumor suppressor genes that occur in *EGFR* (right panel) or *EGFR/TP53* (left panel) mutant human tumors. The relative alteration frequency in *EGFR* or *EGFR/TP53* mutant tumors is reported for genes that were screened in at least 25 tumor samples.
B. Frequency of tumor suppressor gene alterations that co-occur with *ALK* rearrangements and *TP53* mutations in human lung adenocarcinomas (data from AACR Project GENIE). Each bar represents the alteration frequency for each tumor suppressor gene in human lung adenocarcinomas. Interestingly, *ALK*-driven tumors show a strikingly different mutation spectra for tumor suppressor genes, with *SETD2, CDKN2A,* and *APC* being the most commonly co-occurring alterations in this setting, compared to EGFR-driven tumors (Fig. 4D). n.d. = not determined.